ELSEVIER

Earth and Planetary Science Letters 150 (1997) 177–189

EPSL

# Causes and consequences of pressurisation in lava dome eruptions

R.S.J. Sparks *

*Department of Geology, Bristol University, Bristol BS8 1RJ, UK*

Received 9 March 1997; revised 10 June 1997; accepted 12 June 1997

**Abstract**

High total and fluid pressures develop in the interior of high-viscosity lava domes and in the uppermost parts of the feeding conduit system as a consequence of degassing. Two effects are recognised and are modelled quantitatively. First, large increases in magma viscosity result from degassing during magma ascent. Strong vertical gradients in viscosity result and large excess pressures and pressure gradients develop at the top of the conduit and in the dome. Calculations of conduit flow show that almost all the excess pressure drop from the chamber in an andesitic dome eruption occurs during the last several hundred metres of ascent. Second, microlites grow in the melt phase as a consequence of undercooling caused by gas loss. Rapid microlite growth can cause large excess fluid pressures to develop at shallow levels. Theoretically closed-system microlite crystallization can increase local pressure by a few tens of MPa, although build up of pressure will be countered by gas loss through permeable flow and expansion by viscous flow. Microlite crystallization is most effective in causing excess gas pressures at depths of a few hundred metres in the uppermost parts of the conduit and dome interior. Some of the major phenomena of lava dome eruptions can be attributed to these pressurisation effects, including spurts of growth, cycles of dome growth and subsidence, sudden onset of violent explosive activity and disintegration of lava during formation of pyroclastic flows. The characteristic shallow-level, long-period and hybrid seismicity, characteristic of dome eruptions, is attributed to the excess fluid pressures, which are maintained close to the fracture strength of the dome and wallrock, resulting in fluid movement during formation of tensile and shear fractures within the dome and upper conduit. © 1997 Elsevier Science B.V.

*Keywords:* shield volcanoes; pressure; magmas; explosive eruptions; microlite; viscosity

## 1. Introduction

The unpredictable behaviour of growing lava domes is a major problem in volcanology. Lava domes can grow passively and benignly for long periods, but can also generate devastating pyroclastic flows by collapse of unstable domes and can sometimes move into short periods of intense explosive activity. A survey of 156 historic dome eruptions by Newhall and Melson [1] showed that explosive activity occurred in over 95% of cases. Explosions occurred in over half the examples after dome growth began with periods of weeks to many months of extrusion prior to onset of explosive eruption. There is evidence for short-term pulsations in magma discharge rate and, in the case of Lascar Volcano in Chile, subsidence of the lava dome prior to the onset of explosive eruptions [2]. Distinctive shallow-level seismicity associated with lava dome eruptions is often characterised by dominance of long-period fre-

* E-mail: steve.sparks@bristol.ac.uk


*PII* S0012-821X(97)00109-X

quencies [3,4], which has been attributed to resonance of cracks pressurised by high fluid pressures.

In this paper these phenomena are linked to the development of anomalously high pressures within lava domes and in the upper parts of the feeding conduit. The high total and fluid pressures at shallow levels are here attributed to two related factors: first, highly non-linear pressure gradients in the conduit caused by the large vertical viscosity changes that accompany degassing in the ascending magma and, second, microlite crystallization from undercooled melt which may cause large increases in gas pressure. Microlite growth can cause large pressure gradients between the pressurised region and the lava dome above and the magma chamber below. The anomalous pressures and pressure gradients may account for previously unexplained phenomena, such as spurts of growth and pyroclastic flow production, subsidence of the Lascar andesite dome prior to explosive eruption, as well as the occurrence of intense Vulcanian explosions. These effects can also explain the occurrence of distinctive shallow-level seismic activity in growing lava domes and surface degassing phenomena. The concepts developed here are parallel to those developed by Stix et al. [4] for Vulcanian explosions at Galeras Volcano, Colombia, where pressurisation was attributed to microlite crystallization. The concepts provide a framework for developing improved understanding of lava dome behaviour.

## 2. Observations

Observations from several lava dome eruptions indicate that high pressures can develop either in the dome interior or in the upper parts of the conduit beneath the dome. Explosive activity, ranging from short-lived Vulcanian explosions to sustained pumice eruptions, has occurred in many lava dome eruptions [1]. Recent examples include Galeras Volcano, Colombia, in 1992 and 1993 [4], Mount Unzen, Japan, in June 1991 [5], the Soufriere Hills Volcano, Montserrat, on 17 September 1996, and Lascar Volcano, Chile, in 1986, 1989, 1991 and twice in 1993 [2]. The first few episodes of dome growth of Mount St. Helens, Washington, in 1980 involved explosive eruptions in the early stages [6]. The Soufriere Hills Volcano eruption on 17 September 1996 developed into a sustained pumice eruption and the 19–21 April 1993 eruption of Lascar developed into a pulsating pumice eruption involving formation of a short-lived Plinian column and pumice flows [2]. Estimates of internal pressures for explosive eruptions of lava domes are typically in the range 1–20 MPa [2,7–9]. In some examples of Vulcanian explosions the ejecta lithologies indicate that the pressurised source region is within the conduit rather than within the dome. In the case of the Soufriere Hills, Unzen [5] and Galeras [4], the explosions ejected dense glassy rocks and rather dense pumice, but little of the dome rock itself, which is much more crystalline and has intermediate vesicularity to the two Vulcanian ejecta types. Lascar also ejected vesicular pumice and dense glassy rock in the 1986, 1989 and 1991 Vulcanian explosions. Lascar and Soufriere Hills ejecta includes abundant welded breccias, virtrophyres and, in the case of Lascar, partially molten wallrocks [2]. These rocks are interpreted as derived from the shallow conduit and shallow vent walls. Finally in the Galeras eruption the 16 July, 1992 Vulcanian explosion destroyed the dome [4]. Nevertheless there were 5 more Vulcanian explosions in 1993, indicating that overpressure was generated within the conduit, since there was no dome present.

Evidence for development of high gas pressures within lava domes was also apparent in a lobe of the Santiaguito dacite dome, Guatemala, which exploded 3 km from the vent about a year after extrusion had begun [10]. Adilbirov and Dingwell [11] carried out high-temperature experiments on samples of lava dome which were first pressurised and then decompressed in a shock tube. Their experiments indicate that excess internal pressures of a few MPa are required to trigger explosive disintegration of dome rocks. Sato et al. [12] proposed that the spontaneous disintegration of lava fragments, during generation of pyroclastic flows, was the consequence of high internal pore pressures (0.1–1 MPa) within the dome. Fink and Kieffer [13] also proposed that excess explosive pressures are required for the generation of the more violent kinds pyroclastic flow associated with dome growth.

Other evidence for high gas pressures comes from the occurrence of tuffisite veins in both dome rocks and ejected wallrocks from Soufriere Hills and Lascar. Tuffisite veins consist of thin (typically 0.5–5 cm wide) intrusions of fine autoclastic ash, often sintered together. The Mule Creek rhyolitic vent in New Mexico contains networks of the tuffisite veins both in the interior and in the surrounding wallrock [14]. Tuffisite veins are interpreted as hydraulic fractures caused by high fluid pressures in the dome. At Galeras volcano, Colombia [15], and the Soufriere Hills volcano, Montserrat, fine ash-rich jets have been observed emerging from fractures in the dome surface. The jets are often associated with simultaneous long-period earthquakes and are thought to represent venting from pressurised regions in the dome. Tuffisite veins that have been refolded in the interior of lava domes [14] imply further that these hydraulic fractures develop at high temperatures where the magma is also capable of viscous flow.

Long-period (LP) and hybrid earthquakes are characteristic of lava dome eruptions [3,4,15,16]. Some LP earthquakes show almost exact replication of wave forms and swarms of replicate earthquakes can be highly regular. Chouet [3] has interpreted these earthquakes as large surface area resonating cracks, which are repeatedly opened by pressurised fluid. On Galeras a clear link between LP events and degassing has been established from the observations that jets of gas and ash emerge from large cracks on the dome surface simultaneously with LP earthquakes [15]. Other so-called hybrid earthquakes in dome systems combine the high frequencies of volcano-tectonic earthquakes with low-frequency components and can also be interpreted as fracturing in a system with very high fluid pressures, with the movement of fluid influencing the signal [3]. Seismicity at Galeras volcano showed regularities in the increasing number of long-period events, increasing durations of individual signals and decreasing frequencies before an explosive eruption [16], providing a clear link between pressurisation and seismicity. LP earthquakes, assuming they originate from either within the dome or conduit, and tuffisite veins require fluid pressures to exceed the local tensile strength of the magma and for fluid pressure to exceed load pressure.

In many dome eruptions the magma contained high gas contents in the source chamber, but lost a significant amount of this gas during ascent. For example, petrological data, such as presence of hornblende phenocrysts [17] and experimental simulations [18], indicate that the Mount St Helens, Mount Unzen and Soufriere Hills magmas had water contents estimated in the range 4–5 wt%. Barclay et al. [19] have shown that loss or retention of water is the main determinant on the eruption style of peralkaline rhyolites of Mayor Island, New Zealand. Petrological features, such as hornblende reaction rims [20] and extensive groundmass crystallization [21,22], indicate gas loss during ascent. Lava dome eruptions are typically associated with the formation of steam plumes containing juvenile volcanic gases such as $SO_2$ [2,4,23], which also testify to the importance of degassing. Whether extrusive or explosive eruptions occur depends on the rate of gas loss in comparison to the rate of magma ascent [24,25].

## 3. Conduit flow

The most important effect of gas loss during magma ascent is to increase magma viscosity typically by several orders of magnitude. For example, a porphyritic andesite magma at 900°C containing 5 wt% water and a dacitic melt phase has an estimated Newtonian viscosity of $1.3 \times 10^4$ Pa s [26–28]. The same magma partially degassed with 1 wt% water has an estimated viscosity of $(2–4) \times 10^8$ Pa s. Fully degassed, the same magma has an estimated viscosity of $2.6 \times 10^{11}$ Pa s based on observations of movement of a flow lobe of the Soufriere Hills dome. The viscosities may be even higher than these estimates if there has been extensive microlite crystallization and vesiculation, although the effect of crystallization can be countered by concentration of water in the residual melt phase if the system is closed. The more thoroughly degassed and crystallized magma will also develop strongly non-Newtonian properties and mechanical strength, being able to fracture when stress is applied rapidly, but flow when stress is applied more slowly.

Degassing thus creates very large vertical viscosity variations. The largest viscosity changes occur at shallow levels as a consequence of the solubility of water, which depends approximately on the square root of pressure [29] and therefore to a first approximation the square root of depth. The depth dependence of viscosity can be conveniently expressed as a power law:

$$\mu = \mu_0 \exp(-az^n) \quad (1)$$

where $\mu_0$ is the viscosity at the top of the conduit and the function is chosen such that the viscosity at the bottom of conduit is that of the gas-rich magma in the chamber. The parameters $a$, $n$ and $\mu_0$ can be chosen so that they reproduce the pressure-dependent viscosity variations of progressively degassing magma in terms of depth. Some parameterised values of $a$, $n$ and $\mu_0$ for the three models used here to illustrate the principles are listed in Table 1. The models chosen approximately fit the variation of viscosity of porphyritic magma at 900°C and initial water content of 5 wt% ascending from a chamber at 6 km depth. These parameters are a reasonable approximation for conditions in recent dome eruptions such as Unzen, Lascar, Galeras and the Soufriere Hills, Montserrat. Gas is assumed to be lost as the magma rises to the conduit wall. Model 1 assumes that the pressure is approximately magmastatic as a function of depth and that the magma water content is given by the solubility law at the magmastatic pressure. In this parameterisation excess gas is lost as the magma rises. Cases can also be modelled where the pressure is non-magmastatic or the magma is supersaturated to give a depth-dependent function for viscosity. Models 2 and 3 are two examples and are discussed further below. These models provide bounds on behaviour. In real systems variations of conduit cross-sectional area and other parameters

Table 1
Parameters used in three model calculations of excess pressure distribution with depth in conduit flow

| | $n$ | $a$ | $\mu_0$ (Pa s) | $\mu_0\phi$ (Pa s) |
|---|---|---|---|---|
| Model 1 | 0.276 | 10.295 | $2.78\times10^{11}$ | $1.25\times10^{8}$ |
| Model 2 | 0.523 | 3.872 | $2.54\times10^{8}$ | $4.62\times10^{6}$ |
| Model 3 | 0.494 | 4.902 | $1.64\times10^{9}$ | $1.18\times10^{7}$ |

In the table $n$ and $a$ are the coefficients in Eq. (1) describing the depth dependence of magma viscosity. $\mu_0$ is the viscosity at the top of the conduit ($z = 0$) and $\mu_0\phi$ is the effective average viscosity of the magma column. All calculations start at $z = 6$ km and $z$ is in kilometres. Parameters are chosen to be typical of porphyritic andesitic magma at 900°C with an initial water content of 5 wt%.

may lead to second-order variations, but will not change the fundamental features of the models.

Consider a conduit of constant cross-sectional area, sustaining a flow rate $Q$ and driven by an excess pressure $P_e$, defined as the difference between the chamber pressure and the magmastatic pressure. The usual Poiseuille flow law [30] can be modified to give:

$$P(z) = \psi Q \mu_0 \int \exp(-az^n) \mathrm{d}z \quad (2)$$

where $\psi$ is a function of the dimensions and shape of the feeding conduit ($\psi = 8\pi/r^4$ for a cylinder of radius $r$) and $P(z)$ is the excess pressure above the magmastatic pressure gradient at depth $z$. Eq. (2) can be solved by expanding the exponential term into a series and then integrating each term. The resulting Taylor series is slowly converging for typical values of $a$, $n$ and $\mu_0$ that mimic the pressure dependence of viscosity and saturated water contents. Typically between 40 and 60 terms are required for convergence. The value of this series is termed $\phi$. The value $\mu_0\phi$ can be regarded as the effective average viscosity of the column of magma and values are given for the different models in Table 1.

Fig. 1 shows the distribution of excess pressure with depth for models 1, 2 and 3. The excess pressure ratio is given relative to the magma chamber excess pressure as the ratio $P(z)/P_e$, so that the other constant parameters ($\psi Q$) cancel out. Clearly the value of $\psi Q$ has to be compatible with plausible values of chamber pressure. If conduit cross-section varied with height then a more complex model would be required, but a constant cross-sectional area is sufficient to illustrate the underlying principles. The total pressure at any depth can be calculated by adding the excess pressure to the magmastatic pressure if $P_e$ is known.

Model 1 assumes that the magma is completely degassed at 1 atm pressure at the top of the conduit. This is an extreme case. In practise the conduit is likely to flare near the surface and account must be taken of pressures related to the load of the dome and its growth. Some of the degassing and flow takes place in the flared region and the dome. Thus the pressure at the top of the conduit feeding a dome

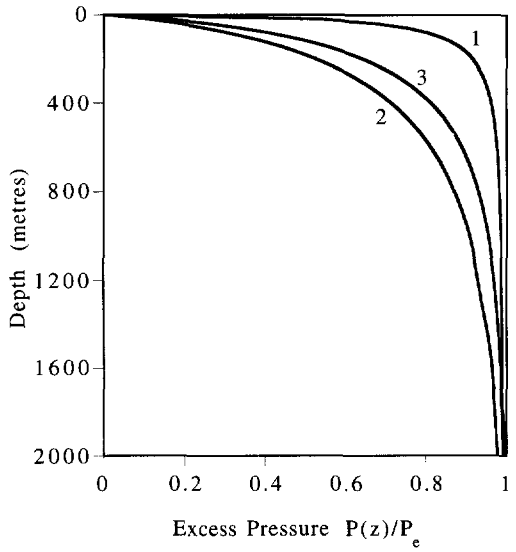


Fig. 1. The variation of excess pressure with depth for the three models listed in Table 1, showing effects of large vertical viscosity gradients in andesite magma as it ascends and degasses. Excess pressure $P(z)$ is normalised by the excess magma chamber pressure $P_e$. The magmastatic pressure must be added to the excess pressure to calculate the total pressure. Only excess pressure variations in the uppermost 2 km are shown, because the excess pressure is almost equal to the excess chamber pressure in the first 4 km of ascent from the chamber at 6 km.

eruption will be much higher than 1 atm due to the magmastatic pressure of the dome and any excess pressure resulting from dome growth. The viscosity at the top of the conduit will typically be significantly lower than the extreme degassed state due to gases dissolved at the conduit exit pressure. Model 2 assumes that the viscosity at the top of the feeding conduit is equivalent to magma containing 1 wt% dissolved water, equivalent to a total pressure of 5.9 MPa. Model 3 was generated by iteration. Viscosity distributions with depth were varied until a pressure distribution was achieved which matched the viscosity of water-saturated magma at each pressure for a value of chamber excess pressure, $P_e = 5$ MPa and an exit total pressure of 2.5 MPa. Model 3 can be envisaged as a case where a lava dome up to 100 m thick is being fed from a conduit and the gas is lost during ascent for magma that just remains gas-saturated at the local pressure.

The calculations show that almost all the pressure drop from the magma chamber to the surface is concentrated at the top of the conduit system and overlying lava dome. Models 2 and 3 are more realistic and show that most of the excess pressure drop from the magma chamber to the surface occurs in the last several hundred metres of ascent. Thus high excess pressures and large pressure gradients are expected in the deep interior of lava domes and in the upper parts of the conduit. Calculations of initial excess pressures in chambers are in the range of 5–20 MPa, comparable to the strength of rocks. For the andesitic lava dome of the Soufriere Hills, Montserrat, the height of the lava dome exceeded 200 m, suggesting chamber excess pressure of at least 5 MPa. Stasiuk et al. [30] estimated initial excess chamber pressures of 10–23 MPa for the three lava eruptions of Lonquimay in Chile in 1989, Soufriere St Vincent in 1979 and Parucutin in Mexico in 1946–1952.

## 4. Microlite crystallization and excess fluid pressures

The high excess pressures near the surface caused by vertical viscosity gradients are sufficient to create large excess fluid pressures compared to the lithostatic pressure in the surrounding wallrocks [25,31]. These large horizontal pressure gradients presumably cause loss of some gas to the wallrocks. There is, however, a second mechanism for achieving very high gas pressures within degassing lava domes: by the growth of microlites from undercooled melt. As magma ascends and loses gas the melt phase becomes undercooled and responds by groundmass crystallization [21,22,32,33]. For example, the solidus of dacite magma containing 5 wt% water increases by about 200°C when completely degassed at constant temperature. As magma ascends and gas is lost microlite crystallization can concentrate the remaining gas in smaller amounts of residual melt and gas bubbles that form as a consequence of supersaturation. Microlite crystallization must lag behind degassing due to the requirement of undercooling for the nucleation and growth of crystals [21,32]. Close to the conduit margins cooling of the magma can also induce undercooling and trigger microlite crystallization.

Tait et al. [34] demonstrated that pressure can increase markedly as a consequence of small amounts of crystallization in a shallow-level magma chamber. These same principles can be applied to groundmass crystallization in the conduits and the interior of lava domes. The potential size of the pressure increase can be illustrated by calculation of the pressure changes that take place during closed-system and constant-volume crystallization of an andesitic magma at 900°C initially containing 35% phenocrysts. In the calculations the density of the system stays constant at 2410 kg $m^{-3}$, the solid crystalline density is chosen as 2650 kg $m^{-3}$ and the melt phase is chosen as constant at 2300 kg $m^{-3}$. It is assumed that the melt phase has become undercooled due to gas loss from an initial water content of 5 wt% in a chamber at a depth of 6 km. In the calculations the solubility of water is assumed to be proportional to the square root of pressure [29] with a solubility constant $S = 4.186 \times 10^{-6}$ $Pa^{-1/2}$. The mass of gas per unit volume, $m_g$, is related to the pressure by the following relationship:

$$m_g = m_m S P^{0.5} + (P/P_i)\rho_i V_{ge} \tag{3}$$

where $m_m$ is the mass of melt per unit volume, $V_{ge}$ is the volume fraction of exsolved gas, $\rho_i$ is a reference gas density, $P$ is the pressure and $P_i$ is a reference pressure. The reference conditions are taken as the density of water at 142.7 MPa and 900°C. The first term on the right-hand side of Eq. (3) is dissolved water and the second term is exsolved water.

Excess pressures are first calculated for groundmass crystallization from an undercooled melt initially saturated with 1% water at the saturation pressure of 5.7 MPa. Fig. 2a shows how excess pressure increases with groundmass crystallization if the volume is held constant and no gas loss takes place. The gas phase is concentrated into residual melt (Fig. 2b) and exsolved gas bubbles (Fig. 2c). The porosity (bubble content) of the system increases as the pressure rises (Fig. 2d), because more of the gas phase exsolves. In a closed system groundmass crystallization will continue until the liquidus of the melt phase is reached and the undercooling goes to zero. There is therefore a limit to the excess pressure that can be reached. Here a relationship between the fraction of crystals in the groundmass and $P_{H_2O}$ is chosen (Fig. 3) to provide some illustrative calculations of the potential for generating excess pressures by degassing and crystallizing magma as a function of depth. For a range of starting water contents of the melt phase from 5% to 0.13%, the amount of groundmass crystallization required to reach the liq-

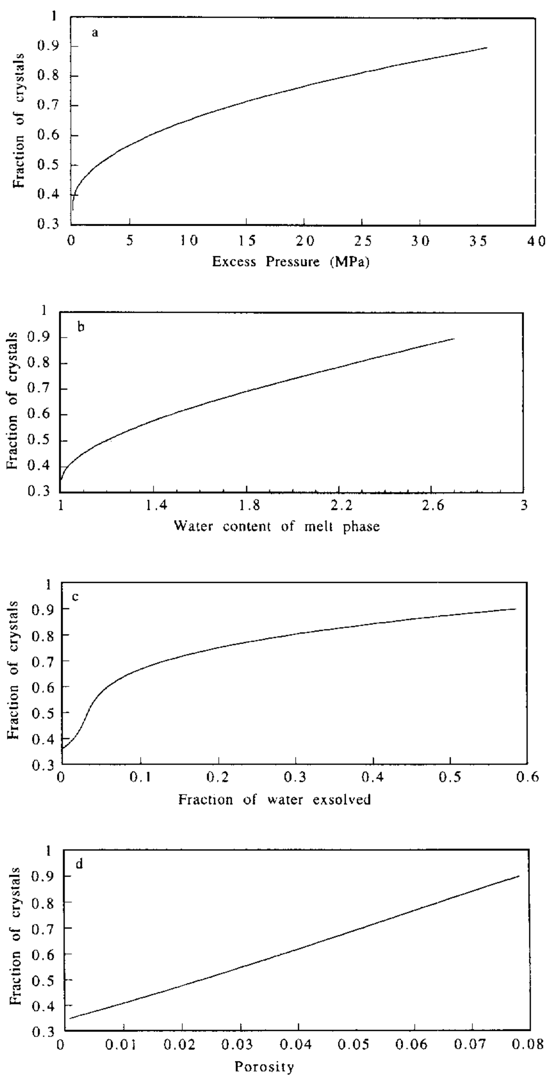


Fig. 2. The variations of excess internal pressure (a), melt water content (b), fraction of water as an exsolved vapour phase (c) and porosity (d) with amount of groundmass crystallization for an andesite magma at 900°C containing 35 wt% phenocrysts and a melt phase containing 1% water. The calculations assume a closed system with no volume change, a melt phase density of 2300 kg $m^{-3}$ and a crystal density of 2650 kg $m^{-3}$. The system is assumed to be initially at a pressure where the melt phase is just saturated at a pressure of 5.7 MPa.

uidus was estimated and then Eq. (3) solved to estimate the total pressure. In the calculations the initial pressure is taken as the saturation pressure at the initial water content in the melt phase before groundmass crystallization. The excess pressure is the difference between the initial pressure and the pressure when equilibrium conditions are attained due to groundmass crystallization.

Fig. 4 shows the theoretical excess pressure as a function of total pressure, displaying a marked maximum at a total pressure of about 23 MPa. At greater depths the increasing solubility of water and compressibility of exsolved water causes the maximum excess pressure to decrease. The excess pressure is zero at 147 MPa total pressure where 5% water is just saturated and there is no undercooling to cause groundmass crystallization. At pressures less than 23 MPa the decreasing initial quantity of water causes the maximum excess pressure to decrease. The excess pressure approaches zero at the surfaces pressures (0.1 MPa total pressure), because there is so little gas present. There is always an excess exsolved vapour phase present, because of the volume change created by the phase change from melt to higher-density solid. The calculations show that excess pressures of tens of MPa are theoretically possible. There is a range of conditions where the effects of groundmass crystallization in developing an excess pressure are at a maximum. In the illustrative calculations the maximum in excess pressure is developed at an initial total pressure (23 MPa) equivalent to a depth of 960 m for a magmastatic pressure regime, but would be considerably shallower for flowing systems with pressure distributions related to dynamic regimes as illustrated in Fig. 1. For an excess chamber pressure of 10 MPa and active conduit flow as in model 1 the depth equivalent of 23 MPa would be about 500 m depth.

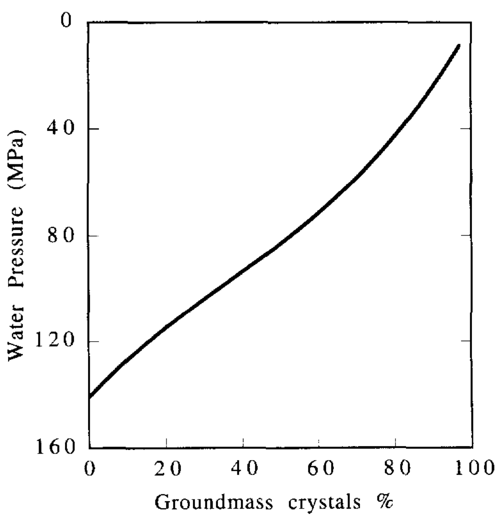


Fig. 3. The relationship between water pressure and equilibrium crystal content as a weight percentage in the groundmass of an andesitic magma at 900°C used in illustrative calculations. The melt phase is saturated in water at each pressure and the water content for a given water pressure can be found from solubility relationships [25].

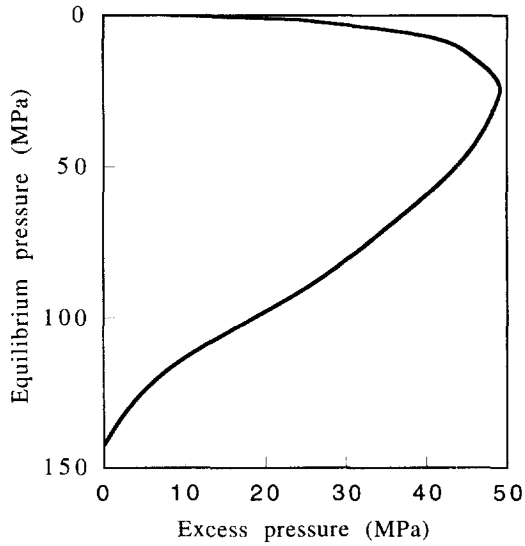


Fig. 4. The variation of total pressure with excess pressure in calculations of the effect of groundmass crystallization in a closed and constant-volume system of andesite magma at 900°C, containing 35% phenocrysts and an initial water content of 5 wt% in the chamber. In the calculations the melt phase has lost some water and so is initially undercooled. The initial water content in the melt phase, prior to groundmass crystallization, ranges from 5 to 0.13 wt% and the initial pressure is the saturation pressure. Groundmass crystallization occurs in the melt phase until the total pressure is at the liquidus using the relationship shown in Fig. 3. The excess pressure is the difference between the initial and final pressure.

These theoretical pressures cannot normally be achieved because of processes that dissipate the build up of gas pressure. First, gas can be lost by permeable flow to the exterior [25,31] or by fracturing the magma and wallrock if the tensile strength is exceeded. Whether high pressures build up will therefore depend on the relative rates of pressure build up due to microlite crystallization and pressure decrease due to permeable gas flow and fracturing. Since the strength of magma and near-surface wallrocks is typically only a few MPa or less the theoretical pressures calculated in Figs. 3 and 4 are unlikely to be attained. Second, the system can adjust by magma flow and expansion. The high pressures that develop due to microlite crystallization can create gradients which expand the magma and drive it away from regions of active microlite crystallization. The ability of magma flow to inhibit the pressure build up will therefore influence whether large excess gas pressures can develop. Third, the calculations also do not take account of elastic deformation of the conduit walls which would result in slightly lower pressures [4,34].

Calculations are presented to provide constraints on these dissipative processes and to evaluate their effectiveness at different depths. In the discussion permeable flow is taken to mean both flow along interconnected vesicles and microfractures and larger-scale flows along fracture networks in the magma and conduit margins. First, the mass percentage of the original gas that must be lost by permeable flow to remain at constant pressure during groundmass crystallization is calculated. Second, the amount of magma expansion expressed as volumetric percentage of vesicles, required to maintain the system at constant pressure and with no gas loss is calculated. Results are shown in Fig. 5. Another constraint can be introduced by calculating the porosity of the melt and gas phase components of the system for the closed-system case. As crystallization takes place the residual melt phase is likely to form a continuous interconnected network in between the microlites. Gas exsolved in this melt phase can become interconnected if volumetric proportion of gas in the interconnected melt phase is high. Fig. 6 plots the volumetric percentage of gas in the melt phase and exsolved gas component as a function of total pressure for the closed-system constant-volume calculations. These results are now referred to in a discussion of depth dependence of the development of excess pressures by microlite crystallization.

At great depths (large total pressures) the porosity of the melt phase is very small (Fig. 6), but only

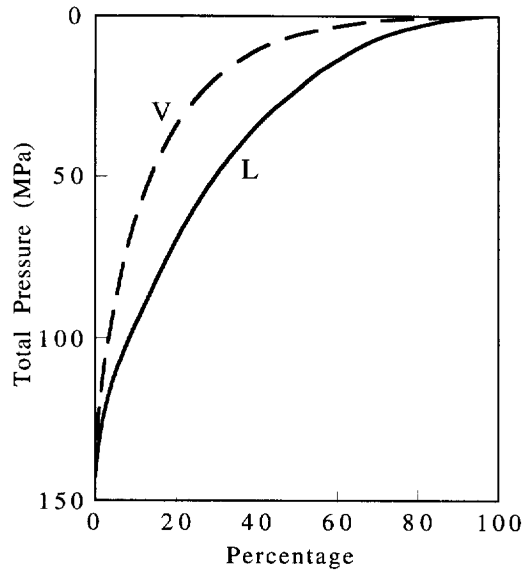


Fig. 5. The percentage of gas that must be lost (curve $L$) or magma expansion that must occur (curve $V$) to maintain a constant pressure during groundmass crystallization is shown as a function of pressure. Gas loss is expressed as the mass percentage of the initial gas content. Magma expansion is shown by the volumetric percentage of vesicles formed during groundmass crystallization. Calculations are carried out for a range of initial water contents in the melt phase from 5 to 0.13 wt% and the pressure is defined as the saturation pressure. Groundmass crystallization is attained, but the pressure is kept constant (no excess pressure develops), implying either continuous gas loss (curve $L$) or expansion of the magma (curve $V$).

small amounts of gas loss or magma expansion are required to avoid pressure build up (Fig. 5). Magma viscosities are low due to high dissolved gas contents, so that the dissipation of excess pressures by viscous flow, bubble expansion [34] and conduit deformation should be effective. The magma is not yet very crystalline at these depths so development of microfractures and fracture networks within the magma are not favoured. Although low porosities indicate low permeabilities undercooling is not possible unless some of the gas is lost by permeable flow [31]. At very shallow levels (low pressures) magma viscosity is very high due to extensive degassing and melt phase porosity is high (Fig. 6). For the viscosities in excess of $10^9$ Pa s that characterise the very shallow region time-scales for readjustments of pressure by bubble expansions are exceedingly slow [35]. The magma is very crystalline and so conditions for developing microfractures and fracture networks by brittle failure are enhanced. These factors favour pressure dissipation by permeable flow over viscous flow and bubble expansion. They also favour fracturing and escape of pressurised gas along them, which may be the major cause of long-period seismicity. This surmise is supported by observation, because lava domes usually erupt with densities much lower than would be the case if expansion were a major factor in accommodating pressure increases and vigorous degassing is observed. Escape of gas is mandatory if undercooling and microlite crystallization are to be triggered [21]. The amount of gas required to be lost or magma expanded increases as depth decreases, but one can infer that gas loss becomes easier close to the surface due to increase in magma permeability, decrease of external pressure and shorter distances for flow.

It is proposed that it is at depths equivalent to the upper parts of the conduit system (0–2 km) and the deep interior of the dome that pressure build up due to microlite crystallization is most effective. In this region the excess pressures can be greatest (Fig. 3), the permeabilities are lower and the magma viscosities high.

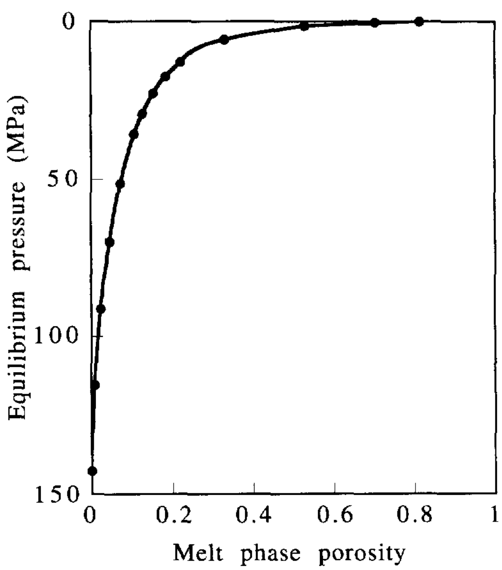


Fig. 6. The melt and exsolved gas phase form an interconnected network in between groundmass microlites. The melt porosity is defined as the volumetric percentage of gas bubbles in the melt and exsolved gas phases and is shown as a function of pressure for the closed-system constant-volume calculations as in Fig. 4.

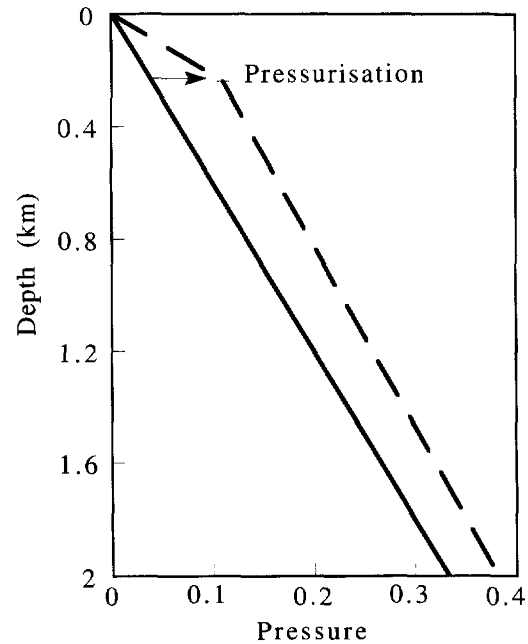


Fig. 7. The variation of pressure with depth resulting from a region of pressurisation developed by closed-system microlite crystallisation in an originally static magma column. The solid line represents the original magmastatic pressure variation with the magma column just balancing the chamber pressure. The dashed lines show schematically the pressure gradients caused by pressurisation by 10 MPa at 240 m depth. The pressure is shown as a fraction of the chamber pressure at 6 km depth. The excess pressure gradients above and below the pressurisation region are positive and negative, respectively.

Gas pressurisation due to microlite growth should be important in static systems. Fig. 7 shows a schematic variation of pressure with depth in a static magma column connected to a lava dome which has reached a height that balances the chamber pressure. This system is conceptualised with the case of Lascar Volcano, Chile, in mind, in which the lava dome is observed to grow in a few months and then remains static and then subsides prior to a major explosive eruption [2]. Matthews et al [2] also observed that fumarolic gas fluxes diminish through a cycle leading to an explosive eruption, implying that gas escape becomes more difficult as the pressure builds up. In the schematic model microlite crystallization in undercooled melt is postulated to take place in the dome interior and upper parts of the conduit. In the illustrative case the excess pressure is allowed to rise to 10 MPa at a depth of about 240 m. Fig. 7 shows that a negative pressure gradient is developed between the region of microlite crystallization and the chamber and a positive gradient occurs above. Thus the pressurisation could result in downward flow back into the chamber.

Gas pressurisation by microlite formation can explain much of the cyclic activity of Lascar. Large excess gas pressures at high levels are required to explain the violent explosive eruptions that ends each cycle. The observed decrease in gas flux in each cycle [2] also implies that gas escape in the system becomes increasingly difficult with time in a cycle. These large pressures cannot be explained by the dynamic pressures related to conduit flow, because the lava dome had stagnated long before the explosion and was in a period of subsidence. The Lascar cycles are characterised by withdrawal of magma down the conduit and surface collapse of the dome [2]. Gas pressurisation can explain the seemingly paradoxical occurrence of pressure build up prior to an explosion and magma withdrawal in two ways. First, the magma may find it easier to flow downwards into the chamber along the negative pressure gradient, because the magma viscosity below the region of pressurisation is much lower than the viscosity of the overlying lava dome. Second, it is possible that the excess pressure reaches a value that exceeds the strength of the wallrock in the upper parts of the conduit, resulting in lateral intrusion of magma and withdrawal at the surface.

Gas pressurisation due to microlite growth can also explain the apparent autoexplosivity of lava domes as they avalanche to form pyroclastic flows [12,13] and explosions of lava flow fronts that have moved well away from the vent [10,36].

## 5. Discussion

This paper presents two causes of high pressures in the interior of lava domes and the uppermost parts of the feeding conduits. Both mechanisms are caused by magmatic degassing, which results in very large changes in magma viscosity and triggers microlite crystallization from the melt phase. The mechanisms can be considered somewhat independently, although there are certainly feedbacks between them and common controlling processes.

The effect of large vertical viscosity gradients is to concentrate almost all the pressure drop between the chamber and the surface to the near-surface environment, typically within the upper several hundred metres of the conduit and interior of the dome. The strength of rocks increases as confining pressure increases and therefore pressures in the chamber that just equal the wallrock strength at depth can exceed the wallrock strength in the near-surface environment. For example, initial chamber excess pressures of 10–20 MPa [30] are much greater than the tensile strength of rocks near the Earth's surface which are unlikely to exceed 3–5 MPa. Degassed viscous magma approaching the surface is therefore capable of easily breaking apart the near-surface rocks and also of forming intrusions as well as extrusions. Excess dynamic pressures will also be matched by equivalent fluid pressures. The fluid pressures in the conduit and dome interior will be substantially greater than the fluid and lithostatic pressures in the surrounding hydrothermal system and wallrock, respectively.

The pressurised gas can flow upwards through the dome itself as illustrated by observations of gas jets from large fractures on the surfaces of active domes [2,15]. However, lateral flow into the conduit wallrocks is likely to be important, since the lateral dimension of the conduit is typically smaller than the vertical height of the overlying dome and conduit. This expectation is born out by observation. Gas loss at Lascar and Galeras is predominantly through fumaroles around the dome margins [2,4]. Thus pressurisation itself provides a potent driving force for gas loss. Sudden pressure drops in the pressurised regions can also explain unexpected explosive eruptions. One cause of sudden pressure drops in dome eruptions is major avalanching, so that explosive eruption follows shortly after a major episode of pyroclastic flow, production as happened on September 17, 1996 at the Soufriere Hills Volcano, Monserrat.

Pressurisation due to viscous effects can only occur during dynamic flow. Lascar Volcano, Chile, and Galeras, Colombia, are cases where pressurisation and explosive eruption occurred during static conditions. Furthermore, sudden decompression due to avalanching cannot be invoked to trigger their explosive episodes. Lascar and Galeras provide evidence that the other mechanism of microlite crystallization is also potent, as this process can occur in a stagnated system. This mechanism requires gas loss that is not completely efficient. A sealed system that losses negligible gas during ascent is expected to erupt entirely explosively [24,25]. A leaky system that losses all its gas efficiently will only form lava, unless some other factor influences behaviour, such as sudden decompression associated with pyroclastic flow activity. The formation of microlites requires some gas loss and undercooling and is intrinsically a disequilibrium process. Pressure build up requires conditions where the loss of pressure by gas flow to the exterior and dissipation of pressure by viscous flow cannot balance the increase in pressure due to microlite crystallization.

The models presented here provide an explanation of the strong seismicity observed at shallow levels in lava dome eruptions. Characteristically seismicity occurs at depths less than 2 km and is concentrated in the upper parts of the conduit and dome interior [3]. There are a variety of earthquake types [3,15,16], but long-period components are often a prominent feature and may relate to resonating fluid-filled fractures [3]. Volcano-tectonic and hybrid earthquakes also imply pressures equivalent to the strength of rock. The models of pressurisation show that excess pressures develop predominantly in the upper several hundred metres of the lava dome systems and thus can account for the shallow character of the seismicity. Large fluid pressures are also predicted and these can account for the evidence of fluid movement and involvement in the seismic signals. The theoretical pressures that are predicted here are much higher than typical rock strengths. These pressures are never likely to be attained because fractures are created at excess pressures equivalent to dome and wallrock strength. Gas is driven out from the crystallizing interior of the dome and conduit along vesicle interconnections and microfractures on the small scale and fracture networks on the large scale. It is speculated that the seismicity is recording this interplay between gas pressure build up, changing mechanical properties of the magma, as degassing and crystallization occurs, and gas loss. The system is maintained at the fracture strength of the wallrocks and dome by the pressurisation processes described here, resulting in the shallow seismicity.

The laws that govern the rate of gas loss from ascending magma, that govern crystal nucleation and growth, and the viscous flow that responds to pressure build up are all likely to be non-linear and difficult to predict in detail. Gas flow is controlled by the permeability distribution in the magma and wallrock and the path length for porous media flow [2,25,31]. Permeability controls in high-temperature magmas are very poorly known and are anticipated to be strongly non-linear functions of porosity [37] and the fracturing properties of high-temperature crystal-rich magma. Crystal nucleation and growth typically involves laws where rates are related to undercooling by a non-linear functions [22,38]. Viscosity variations are also strongly dependent on dissolved gas content and crystal content. There must therefore be complex feedbacks between microlite crystallization, gas loss, viscous flow and fracturing with opportunities for self-excitation of the system. There will also be further complexity added by other processes such as cooling of the magma in the conduit and dome, changes of magma composition, elastic responses in the wallrock, changes to the conduit geometry and changes to the surrounding hydrothermal system.

A major conclusion of this analysis of pressurisation is that lava dome phenomena are mostly controlled by shallow-level processes related to degassing. This highly non-linear system presents challenges to experimentalists, modellers and seismologists. Experimentalists will need to establish better data on rate controlling parameters and processes, such as the permeability of high-temperature magma and the kinetics of crystallization from high-viscosity undercooled melts and on rheological and mechanical properties of highly crystalline magmas. Modellers will need to incorporate the various non-linear processes into models and to explore the inherent strong feedbacks in lava dome systems. Seismologists will need to develop an understanding of the different kinds of earthquakes in the context of the processes described in this paper. Development of the concepts outlined here may help to understand phenomena such as pulsation of lava dome growth, pyroclastic flow production, sudden onset of explosive activity, seismicity during dome growth and fluctuations in gas flux.

## Acknowledgements

These ideas are stimulated by observing the eruptions of Lascar Volcano and the Soufriere Hills Volcano, Montserrat, and discussing the eruption of Mount Unzen with Professors Nakada and Shimizu. The staff at the Montserrat Volcano Observatory are particularly acknowledged for their contributions to documenting the Soufriere Hills eruption. I have also enjoyed numerous discussions with many colleagues on the problems of degassing of magma and lava dome behaviour. Discussions with John Stix, Bernard Chouet and their reviews of this paper were particularly helpful. Research supported by NERC grants GR3/10679 and GR3/9047 and the Leverhulme Trust grant F/182/AL. *[FA]*

## References

[1] C.G. Newhall, W.G. Melson, Explosive activity associated with the growth of volcanic domes, J. Volcanol. Geotherm. Res. 17 (1983) 111–131.

[2] S.J. Matthews, M.C. Gardeweg, R.S.J. Sparks, The 1984–1996 cyclic activity of Lascar Volcano, Northern Chile: cycles of dome growth, dome subsidence, degassing and explosive eruptions, Bull. Volcanol. (in press).

[3] B.A. Chouet, Long-period volcano seismicity — its source and use in eruption forecasting, Nature (London) 380 (1996) 309–316.

[4] J. Stix, R.C. Torres, M.L. Narvaez, G.P. Cortés, J.A. Raigosa, D.M. Gomez, R. Castonguay, A model of Vulcanian eruptions at Galeras Volcano, Colombia, J. Volcanol. Geotherm. Res. 77 (1997) 285–304.

[5] S. Nakada, Lava domes and pyroclastic flows of the 1991–1992 eruption at Unzen volcano, In: T. Yanagi, H. Okada, T. Ohta (Eds.), Unzen Volcano: The 1990–1992 Eruption, Nishinippon and Kyushu University Press, 1993, pp. 56–66.

[6] D.A. Swanson, R.T. Holcomb, Regularities in the growth of the Mount St Helens dacite dome 1980–86, in: J.H. Fink (Ed.), Lava Flows and Domes: Emplacement Mechanisms and Hazard Implications, Springer, Berlin, 1990, pp. 3–24.

[7] S.A. Fagent, L. Wilson, Explosive volcanic eruptions, VII. The ranges of pyroclastic ejected in transient volcanic explosions, Geophys. Int. 113 (1993) 359–370.

[8] S.M. Bower, A.W. Woods, On the dispersal of clasts from volcanic craters during explosive eruptions, J. Volcanol. Geotherm. Res. 73 (1996) 19–32.

[9] L. Mastin, Thermodynamics of gas and steam blast eruptions, Bull. Volcanol. 57 (1995) 85–88.

[10] W.I. Rose, Pattern and mechanism of volcanic activity at Santiaguito volcanic dome, Guatemala, Bull. Volcanol. 37 (1973) 73–94.

[11] M.A. Adilbirov, D.B. Dingwell, Magma fragmentation by rapid decompression, Nature (London) 380 (1996) 146–148.

[12] H. Sato, T. Fujii, S. Nakada, Crumbling of dacite dome lava and generation of pyroclastic flows at Unzen Volcano, Nature (London) 360 (1992) 664–666.

[13] J.H. Fink, S.W. Kieffer, Estimate of pyroclastic flow velocities resulting from explosive decompression of lava domes, Nature (London) 363 (1993) 612–615.

[14] M.V. Stasiuk, J. Barclay, M.R. Carroll, C. Jaupart, J.C. Ratte, R.S.J. Sparks, S.R. Tait, Decompression of volatile-saturated rhyolitic magma in the Mule Creek vent, New Mexico, U.S.A., Bull. Volcanol. 58 (1996) 117–130.

[15] F. Gil Cruz, B.A. Chouet, Long-period events, the most characteristic seismicity accompanying the emplacement and extrusion of a lava dome in Galeras Volcano, Colombia in 1991, J. Volcanol. Geotherm. Res. 77 (1997) 121–158.

[16] R.C. Torres, D.M. Gomez, L.M. Narvaez, Unusual seismic signals associated with activity at Galeras volcano, Colombia, from July 1992 to September 1994, Ann. Geofis. 39 (1996) 299–310.

[17] M.J. Rutherford, J.D. Devine, The May 18, 1980 eruption of Mount St. Helens, 3. Stability and chemistry of amphibole in the magma chamber, J. Geophys. Res. 93 (1988) 11949–11959.

[18] M.J. Rutherford, H. Sigurdsson, S.N. Carey, A.N. Davis, The May 18, 1980 eruption of Mount St. Helens, I. Melt composition and experimental phase equilibria, J. Geophys. Res. 90 (1985) 2929–2947.

[19] J. Barclay, M.R. Carroll, B.F. Houghton, C.J.N. Wilson, Pre-eruptive volatile content and degassing history of an evolving peralkaline volcano, J. Volcanol. Geotherm. Res. 74 (1996) 75–87.

[20] M.J. Rutherford, P.M. Hill, Magma ascent rates from amphibole breakdown: an experimental study applied to the 1980–86 Mount St. Helens eruption, J. Geophys. Res. 98 (1993) 19667–19685.

[21] S.E. Swanson, M.T. Naney, H.R. Westrich, J.C. Eichelberg, Crystallization history of obsidian dome, Inyo domes, California, Bull. Volcanol. 51 (1989) 161–176.

[22] K.V. Cashman, Groundmass crystallization of Mount St. Helens dacite, 1980–86: a tool for interpreting shallow magmatic processes, Contrib. Mineral. Petrol. 99 (1992) 431–449.

[23] R.J. Andres, W.I. Rose, Kyle, P.R., S. de Silva, P.W. Francis, M.C. Gardeweg, R.H. Moreno, Excessive sulfur dioxide emissions from Chilean volcanoes, J. Volcanol. Geotherm. Res., 46 (1991) 323–329; and P.J. Wallace, T.M. Gerlach, Magmatic vapor source for sulfur dioxide released during volcanic eruptions: evidence from Mount Pinatubo, Science 265 (1994) 497–499.

[24] C. Jaupart, C.J. Allegre, Gas content, eruption rate and instabilities in silicic volcanoes, Earth Planet. Sci. Lett. 102 (1991) 413–429.

[25] A.W. Woods, T. Koyaguchi, Transitions between explosive and effusive volcanic eruptions, Nature (London) 370 (1995) 641–644.
[26] H.R. Shaw, Obsidian–$H_2O$ viscosities at 100 and 2000 bars in the temperature range 700 to 900°C, J. Geophys. Res. 68 (1963) 6337–6343.
[27] A.M. Lejeune, P. Richet, Rheology of crystal-bearing silicate melts: an experimental study at high viscosities, J. Geophys. Res. 100 (1995) 4215–4229.
[28] P. Richet, A.M. Lejeune, F. Holtz, J. Roux, Water and the viscosity of andesite melts, Chem. Geol. 128 (1996) 185–197.
[29] E. Stolper, Water in silicate glasses: an infrared spectroscopic study, Contrib. Mineral. Petrol. 81 (1992) 1–17.
[30] M.V. Stasiuk, C. Jaupart, R.S.J. Sparks, On the variations of flow rate in non-explosive lava eruptions, Earth Planet. Sci. Lett. 114 (1993) 505–516.
[31] J.C. Eichelberger, C.R. Carrigan, H.R. Westrich, R.H. Price, Non-explosive silicic volcanism, Nature (London) 323 (1986) 598–602.
[32] R.S.J. Sparks, H. Pinkerton, Effect of degassing on rheology of basaltic magma, Nature (London) 276 (1978) 385–386.
[33] C.H. Geschwind, M.J. Rutherford, Crystallization of microlites during magma ascent: the fluid mechanics of 1980–1986 eruptions at Mount St Helens, Bull. Volcanol. 57 (1995) 356–379.
[34] S.R. Tait, C. Jaupart, S. Vergniolle, Pressure, gas content and eruption periodicity of a shallow crystallizing magma chamber, Earth Planet. Sci. Lett. 92 (1989) 107–123.
[35] J. Barclay, D.S. Riley, R.S.J. Sparks, Analytical models for bubble growth during decompression of high viscosity magmas, Bull. Volcanol. 57 (1995) 422–431.
[36] J.H. Fink, S.W. Anderson, C.R. Manley, Textural constraints on effusive silicic volcanism: beyond the permeable foam model, J. Geophys. Res. 97 (1993) 9073–9083.
[37] H.R. Westrich, J.C. Eichelberger, Gas transport and bubble collapse in rhyolitic magmas: an experimental approach, Bull. Volcanol. 56 (1994) 447–458.
[38] G.F. Lofgren, Experimental studies on the dynamic crystallization of silicate melts, in: R.B. Hargreaves (Ed.), The Physics of Magmatic Processes, Princeton University Press, Princeton, NJ, 1980, pp. 487–551.